

Implications of the 125 GeV Higgs for Supersymmetry

Sabine Kraml

Laboratoire de Physique Subatomique et de Cosmologie, UJF Grenoble 1,
CNRS/IN2P3, INPG, 53 Avenue des Martyrs, F-38026 Grenoble, France

The current LHC Higgs results may be used as a guide for where to look for SUSY. This contribution discusses implications of the 125 GeV Higgs boson for the MSSM and NMSSM. Using boundary conditions at the GUT scale, gluinos and light-flavor squarks turn out to be heavy, in accordance with the current SUSY search limits, while stops can still be light, below 1 TeV. The observed Higgs signal is much easier accommodated in the NMSSM than in the MSSM. Particularly interesting are NMSSM scenarios with large λ and small $\tan\beta$: they are characterized by light stops and light higgsinos, and offer the intriguing possibilities of, e.g., observing a second light Higgs boson with lower mass, or two (quasi-)degenerate Higgs bosons near 125 GeV.

1 Introduction

The recent discovery [1, 2] of a new particle with mass around 125 GeV and properties consistent with a Standard Model (SM) Higgs boson is a first triumph for the LHC physics program. However, while this discovery completes our picture of the SM, it still leaves many fundamental questions open. One of the most pressing issues is that the SM does not explain the value of the electroweak (EW) scale itself: Why is the Higgs boson so light when it is predicted to be driven to the scale of Grand Unified Theories (M_{GUT}), or even the Planck scale, by radiative corrections? Either new physics appears at the EW scale, or the Higgs mass-squared is fine tuned at the 10^{-32} level.

New particles that couple to the Higgs can however also modify the Higgs couplings, and thus the production and decay rates in various channels. So on the one hand we expect physics beyond the SM (BSM) to explain the Higgs mass, on the other hand the measured mass and signal strengths provide significant constraints on concrete BSM realizations, see *e.g.* [3, 4]. Moreover, while the SM provides a reasonably good fit to the current data, based on the results published in 2012, some new physics contributions to the effective Higgs couplings to gluons and photons are preferred, as shown in Fig. 1.¹

The arguably best motivated extension of the SM is weak-scale supersymmetry (SUSY), introducing a new symmetry between fermions and bosons. SUSY solves the hierarchy problem provided SUSY particles exist

¹Based on the experimental results available at the end of 2012.

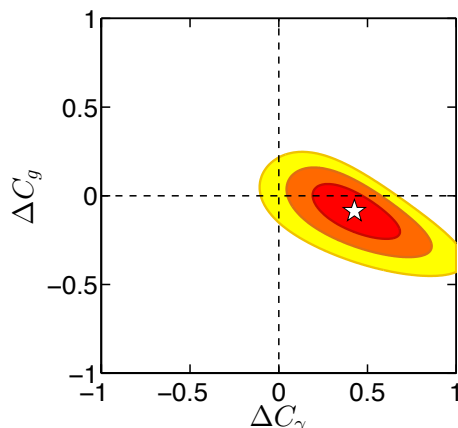


Figure 1: Global fit of additional loop contributions ΔC_g and ΔC_γ from new particles to the Higgs couplings to gluons and photons, assuming SM values for the couplings to W, Z and SM fermions. The fit includes all available Higgs signal strengths from ATLAS, CMS and the Tevatron experiments. The red, orange and yellow ellipses show the 68%, 95% and 99.7% CL regions, respectively. The white star marks the best-fit point $\Delta C_g = -0.086$, $\Delta C_\gamma = 0.426$. From [4].

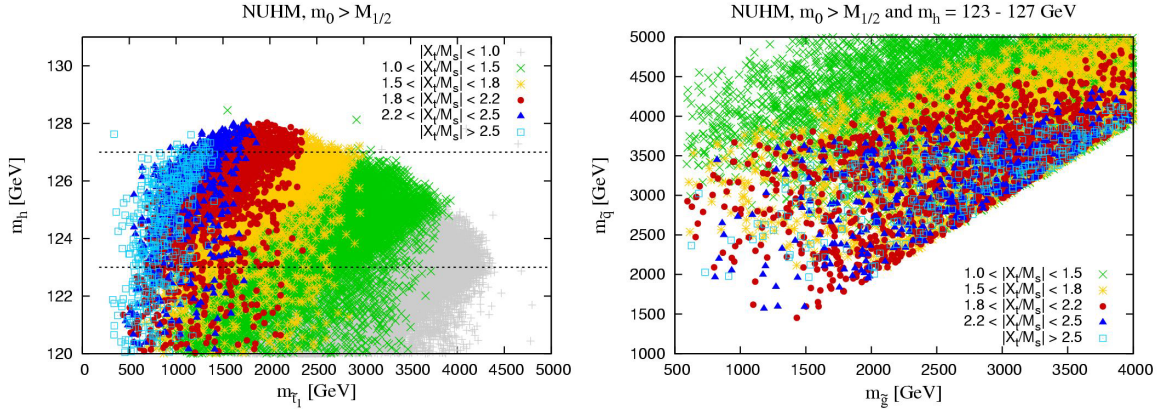


Figure 2: Left: dependence of m_h on $m_{\tilde{t}_1}$ in the NUHM model, with the amount of stop mixing indicated by a color code. Right: projection of the points with $m_h = 123\text{--}127$ GeV in the squark versus gluino mass plane. From [6].

at or around the TeV energy scale. The (Next-to-) Minimal Supersymmetric Standard Model, (N)MSSM, moreover predicts a light, often SM-like, Higgs boson with mass below ≈ 135 (140) GeV. This has always been regarded as an intriguing feature, and even more so with the actual observation of a Higgs-like state at 125 GeV. So far, however, SUSY searches at ATLAS and CMS show no signal whatsoever, and the mass limits in particular for squarks and gluinos have been pushed well into the TeV range [7, 8].

So the Higgs has been found — but where is supersymmetry? In fact, the SUSY particles relevant for the Higgs sector and the hierarchy problem, stops and higgsinos, are much less constrained than light-flavor squarks and gluinos. “Natural” SUSY still lives on. In this talk I therefore discuss some implications of the LHC Higgs results for supersymmetric models.

2 Minimal Supersymmetric Standard Model

In the MSSM, $m_h^2 = m_Z^2 \cos^2 2\beta$ at tree level, where $\tan \beta = v_u/v_d$, $v = \sqrt{v_u^2 + v_d^2} = 174$ GeV. This quickly saturates to $m_h^2 \lesssim m_Z^2$ for $\tan \beta \gtrsim 5$. To further lift m_h^2 from $m_Z^2 = (91 \text{ GeV})^2$ to around $(125 \text{ GeV})^2$, radiative corrections nearly as large as the tree-level value are required. The leading one-loop correction comes from the top–stop sector and is given by [5]

$$\Delta m_h^2 = \frac{3}{4\pi^2} \frac{m_t^4}{v^2} \left(\log \frac{M_S^2}{m_t^2} + \frac{X_t^2}{M_S^2} \left(1 - \frac{X_t^2}{12 M_S^2} \right) \right). \quad (1)$$

Here m_t is the running top-quark mass at the scale m_t , $M_S^2 = m_{\tilde{t}_1} m_{\tilde{t}_2}$ with $m_{\tilde{t}_{1,2}}$ the stop masses, and X_t is the stop mixing parameter, $X_t = A_t - \mu \cot \beta$, at the scale M_S . The contribution from the logarithmic term in Eq. (1) can be increased by simply raising M_S , but naturalness demands that the SUSY scale should be not too far above the EW scale. The X_t contribution is maximized at $|X_t/M_S| \simeq \sqrt{6} = 2.45$; this is called the maximal-mixing scenario.

As a consequence, $m_h \simeq 125$ GeV requires either (unnaturally) heavy stops, or maximal mixing. This is illustrated in Fig. 2 for a semi-constrained version of the MSSM with universal gaugino mass $M_{1/2}$, scalar mass m_0 and trilinear coupling A_0 all defined at M_{GUT} , but non-universal Higgs mass parameters (NUHM model). As can be seen, a 125 GeV Higgs together with stops in the 0.5–1 TeV mass range indeed requires maximal mixing, *i.e.* very large $|A_t|$ (left plot). At the same time, gluinos and 1st/2nd generation squarks turn out to be heavy, with masses above 1–2 TeV (right plot), thus automatically avoiding the current LHC limits. The Higgs signal strengths in the $\gamma\gamma$ and ZZ channels are however typically $R \lesssim 1$, see [6].

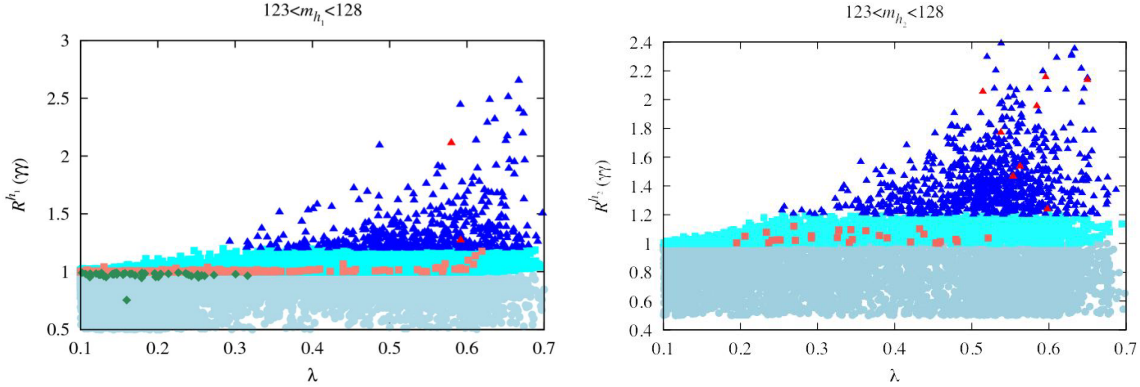


Figure 3: Signal strength (relative to SM) in the $h_i \rightarrow \gamma\gamma$ channel as function of λ from a scan over the semi-constrained NMSSM, on the left for the h_1 lying in the 123 – 128 GeV mass range, on the right for the h_2 lying in the 123 – 128 GeV range. See text for color code.

3 Next-to-Minimal Supersymmetric Standard Model

The NMSSM differs from the MSSM by to the presence of the gauge singlet superfield \hat{S} [9]. In the simplest Z_3 invariant realization of the NMSSM, the Higgs mass term $\mu \hat{H}_u \hat{H}_d$ in the superpotential W_{MSSM} of the MSSM is replaced by the coupling λ of \hat{S} to \hat{H}_u and \hat{H}_d and a self-coupling κS^3 . The superpotential W_{NMSSM} is given by:

$$W_{\text{NMSSM}} = \lambda \hat{S} \hat{H}_u \cdot \hat{H}_d + \frac{\kappa}{3} \hat{S}^3 + \dots, \quad (2)$$

where hatted letters denote superfields, and the dots denote the MSSM-like Yukawa couplings of \hat{H}_u and \hat{H}_d to the quark and lepton superfields. Once the real scalar component of \hat{S} develops a vev $\langle S \rangle$, the first term in W_{NMSSM} generates an effective μ -term, $\mu_{\text{eff}} = \lambda \langle S \rangle$.

As compared to two independent parameters in the Higgs sector of the MSSM at tree level, often chosen as $\tan\beta$ and M_A , the Higgs sector is now described by

$$\lambda, \kappa, A_\lambda, A_\kappa, \tan\beta = v_u/v_d, \mu_{\text{eff}}. \quad (3)$$

The neutral Higgs sector of this model consists of three CP-even (h_1, h_2, h_3) and two CP-odd (a_1, a_2) states. The CP-even mass eigenstates are superpositions of the neutral CP-even components of H_u, H_d, S :

$$\begin{aligned} h_1 &= \mathcal{S}_{1,d} H_d + \mathcal{S}_{1,u} H_u + \mathcal{S}_{1,s} S, \\ h_2 &= \mathcal{S}_{2,d} H_d + \mathcal{S}_{2,u} H_u + \mathcal{S}_{2,s} S, \\ h_3 &= \mathcal{S}_{3,d} H_d + \mathcal{S}_{3,u} H_u + \mathcal{S}_{3,s} S, \end{aligned} \quad (4)$$

with the couplings to gauge bosons and fermions determined by the 3×3 mixing matrix \mathcal{S} , *e.g.* $g_{h_i VV} / g_{H_{\text{SM}} VV} = \cos\beta \mathcal{S}_{i,d} + \sin\beta \mathcal{S}_{i,u}$.

An interesting feature is that the coupling $\lambda S \hat{H}_u \hat{H}_d$ in the superpotential leads to an extra tree-level contribution to the SM-like Higgs mass $m_h^2 = m_Z^2 \cos^2 2\beta + \lambda v^2 \sin^2 2\beta + \Delta m_h^2$. It is thus much easier to obtain $m_h \simeq 125$ GeV in constrained versions of the NMSSM than in their MSSM equivalents [10]. Moreover, as pointed out by Ellwanger [11, 12], for large λ (and small $\tan\beta$) doublet–singlet mixing can reduce the hbb coupling, thus enhancing the di-photon signal at the LHC. This works in fact for both, the lightest and the second-lightest scalar, h_1 and h_2 , and either of them could be the observed state at 125 GeV [12, 10, 13].

For illustration, Fig. 3 shows the result of a scan of the “semi-constrained” NMSSM with universal $m_0, M_{1/2}$ and A_0 at the GUT scale, but the NMSSM-specific parameters of Eq. (3) treated as free parameters at the EW scale. The scan was performed with `NMSSMTools` [14]; all points have a neutralino as the lightest SUSY particle (LSP) and obey the current mass limits as well as the constraints on $\text{BR}(B_s \rightarrow X_s \gamma), \Delta M_s$,

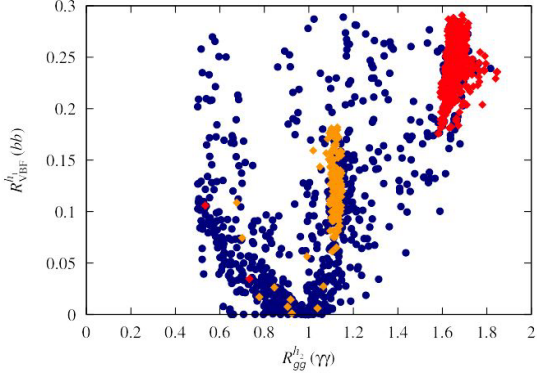


Figure 4: Signal strengths (relative to SM) $R_{\text{VBF}}^{h_1}(b\bar{b})$ versus $R_{gg}^{h_2}(\gamma\gamma)$ for $m_{h_1} \in [96, 100]$ GeV and $m_{h_2} \in [123, 128]$ GeV in the semi-constrained NMSSM. Blue points have $\Omega h^2 < 0.094$ while red and orange points have $\Omega h^2 \in [0.094, 0.136]$. From [15].

ΔM_d , $\text{BR}(B_s \rightarrow \mu^+\mu^-)$, $\text{BR}(B^+ \rightarrow \tau^+\nu_\tau)$ and $\text{BR}(B \rightarrow X_s\mu^+\mu^-)$ at 2σ . The light, medium and dark blue points have $\Omega h^2 \leq 0.136$ and obey the bounds on the spin-independent LSP–proton scattering cross section from XENON100. Light and medium red points have $0.094 \leq \Omega h^2 \leq 0.136$ and of course also pass the XENON100 bounds. (The shades of blue and red just help indicate the level of enhancement or suppression of the $\gamma\gamma$ signal.) The green points have $\Omega h^2 \leq 0.136$ and in addition explain Δa_μ within 2σ .

4 Two Higgs bosons at 98 and 125 GeV

If the h_2 of the NMSSM is responsible for the signal at 125 GeV, a particularly interesting question [15] is whether one could simultaneously explain the LHC signal and the small ($\sim 2\sigma$) LEP excess in $e^+e^- \rightarrow Zb\bar{b}$ in the vicinity of $M_{b\bar{b}} \sim 98$ GeV. We recall that the LEP excess is clearly inconsistent with a SM-like Higgs boson at this mass, being only about 10 – 20% of the rate predicted for the H_{SM} . Consistency with such a result for the h_1 is natural if the h_1 couples at a reduced level to ZZ , which, in turn, is automatic if the h_2 has substantial ZZ coupling, as required by the observed LHC signals.

As above, we perform a scan over the semi-constrained NMSSM. We compute the ratio of the gg or VBF induced Higgs cross section times the Higgs branching ratio to a given final state X , relative to the corresponding value for the SM Higgs boson, as²

$$R_{gg}^{h_i}(X) \equiv \frac{\Gamma(h_i \rightarrow gg) \text{BR}(h_i \rightarrow X)}{\Gamma(H_{\text{SM}} \rightarrow gg) \text{BR}(H_{\text{SM}} \rightarrow X)}, \quad R_{\text{VBF}}^{h_i}(X) \equiv \frac{\Gamma(h_i \rightarrow WW) \text{BR}(h_i \rightarrow X)}{\Gamma(H_{\text{SM}} \rightarrow WW) \text{BR}(H_{\text{SM}} \rightarrow X)}, \quad (5)$$

where h_i is the i^{th} NMSSM scalar Higgs, and H_{SM} is the SM Higgs boson, taking $m_{H_{\text{SM}}} = m_{h_i}$.

To describe the LEP and LHC data the h_1 and h_2 must have $m_{h_1} \sim 98$ GeV and $m_{h_2} \sim 125$ GeV, respectively, with the h_1 being largely singlet and the h_2 being primarily doublet (mainly H_u for the scenarios we consider). Figure 4 shows $R_{\text{VBF}}^{h_1}(b\bar{b})$ versus $R_{gg}^{h_2}(\gamma\gamma)$ for the scan points that pass LEP, B -physics and dark matter constraints as above and have in addition $m_{h_1} \in [96, 100]$ GeV and $m_{h_2} \in [123, 128]$ GeV. (These ranges take into account a 2–3 GeV theoretical error in the computation of the Higgs masses.) The points with $0.1 \leq R_{\text{VBF}}^{h_1}(b\bar{b}) \leq 0.25$ would provide the best fit to the LEP excess. As can be seen, a large portion of these points have $R_{gg}^{h_2}(\gamma\gamma) > 1$ as preferred by LHC data.

In the following we thus require $m_{h_1} \in [96, 100]$ GeV with $0.1 \leq R_{\text{VBF}}^{h_1}(b\bar{b}) \leq 0.25$, and $m_{h_2} \in [123, 128]$ GeV with $R_{gg}^{h_2}(\gamma\gamma) > 1$. We refer to this as the “98 + 125 GeV Higgs scenario”. Points with $\Omega h^2 < 0.094$ are represented by blue circles and points with $\Omega h^2 \in [0.094, 0.136]$ (the “WMAP window”) are represented by red/orange diamonds.

Two distinct WMAP-window regions appear. The red region has $R_{gg}^{h_2}(\gamma\gamma) \sim 1.6$ and corresponds $\mu_{\text{eff}} \sim 120$ GeV and $\tan \beta \sim 2$; as can be seen in Fig. 5, it features a partly light spectrum with $m_{\tilde{\chi}_1^0} \sim 70 - 80$ GeV, $m_{\tilde{\chi}_1^\pm} \sim 105 - 110$ GeV and $m_{\tilde{t}_1} \sim 0.2 - 1$ TeV, while $m_{\tilde{g}} \gtrsim 1$ TeV and $m_{\tilde{q}} \gtrsim 2$ TeV. Again, LHC SUSY limits are automatically avoided by the Higgs-sector requirements. Moreover, the other Higgses are light,

²Note that $R_{\text{VBF}}^{h_1}(b\bar{b})$ is equivalent to $R_{Vh_1}^{h_1}(bb)$ as relevant for LEP.

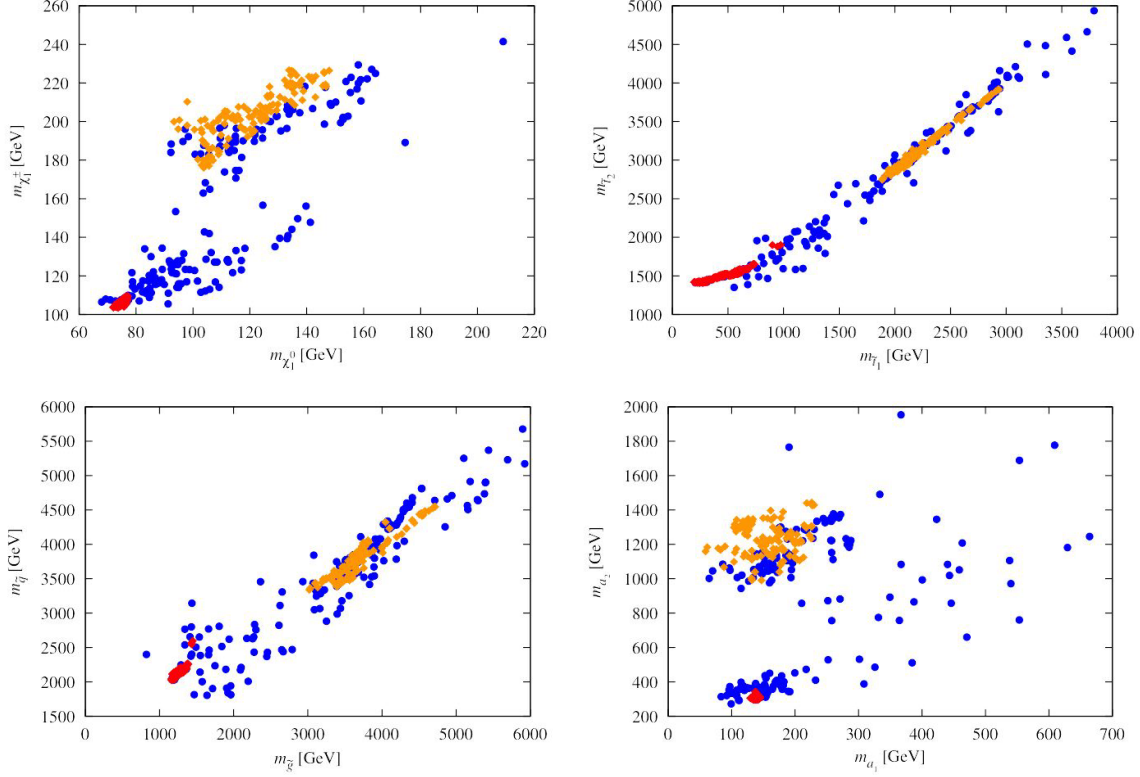


Figure 5: Expectations for sparticle and Higgs masses in the 98 + 125 GeV Higgs scenario. Blue points have $\Omega h^2 < 0.094$ while red and orange points have $\Omega h^2 \in [0.094, 0.136]$. From [15].

too, $m_{a_2} \sim 150$ GeV and $m_{h_3} \simeq m_{H^\pm} \simeq m_{a_2} \sim 300 - 400$ GeV. The orange region is quite different. It appears at $\mu_{\text{eff}} \sim 200$ GeV and $\tan \beta \sim 5 - 8$ and has $R_{gg}^{h_2}(\gamma\gamma) \sim 1.1$. The overall mass scale is much heavier: $m_{\tilde{\chi}_1^0} \sim 90 - 150$ GeV and $m_{\tilde{t}_1} > 1.8$ TeV, see Fig. 5. Squarks and gluinos lie in the 3 – 5 TeV mass range, above the reach of the 14 TeV LHC. The heavy Higgses also have masses above 1 TeV, only the a_1 is still light with $m_{a_1} \lesssim 250$ GeV.

The LSP decomposition and its expected spin-independent scattering cross section off protons are shown in Fig. 6. The prospects to test the 98 + 125 GeV Higgs scenario at the LHC and a future ILC are discussed in detail in [15]. Obviously the ILC would be the ideal machine to explore the light charginos and neutralinos present in this scenario, and to precisely measure their properties.

An e^+e^- collider would also be the ideal machine to produce the additional Higgs states. Production cross sections for the various Higgs final states are shown in Fig. 7 for three illustrative scenarios specified in Table 1 taken from our NMSSM scans. The first plot is for a WMAP-window scenario with $m_{\tilde{\chi}_1^0} \sim 76$ GeV and light Higgs bosons. The third plot is for the point in region B with smallest m_{h_3} , for which $m_{a_2}, m_{h_3}, m_{H^\pm}$ are all around 1 TeV. The second plot is for a sample scenario with Higgs masses that are intermediate, as only possible if Ωh^2 lies below the WMAP window. With an integrated luminosity of 1000 fb^{-1} , substantial event rates for many Z +Higgs and Higgs pair final states are predicted. In the e^+e^- collider case, it would be easy to isolate signals in many final states. For example, in the case of Higgs pairs, final states such as $(t\bar{t})(t\bar{t})$, $(\tilde{\chi}_1^0\tilde{\chi}_1^0)(t\bar{t})$ and so forth could be readily identified above background. Observation of the $(\tilde{\chi}_1^0\tilde{\chi}_1^0)(\tilde{\chi}_1^0\tilde{\chi}_1^0)$ final states would require a photon tag and would thus suffer from a reduced cross section. Associated Z +Higgs, with Higgs decaying to $t\bar{t}$ or $\tilde{\chi}_1^0\tilde{\chi}_1^0$ would be even more readily observed.

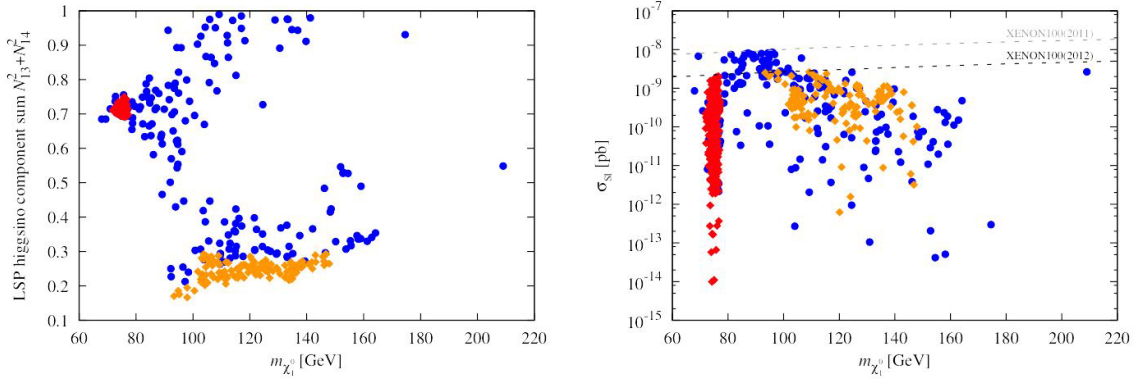


Figure 6: LSP higgsino component (left) and spin-independent scattering cross section (right) as function of the LSP mass for the 98 + 125 GeV Higgs scenarios. From [15].

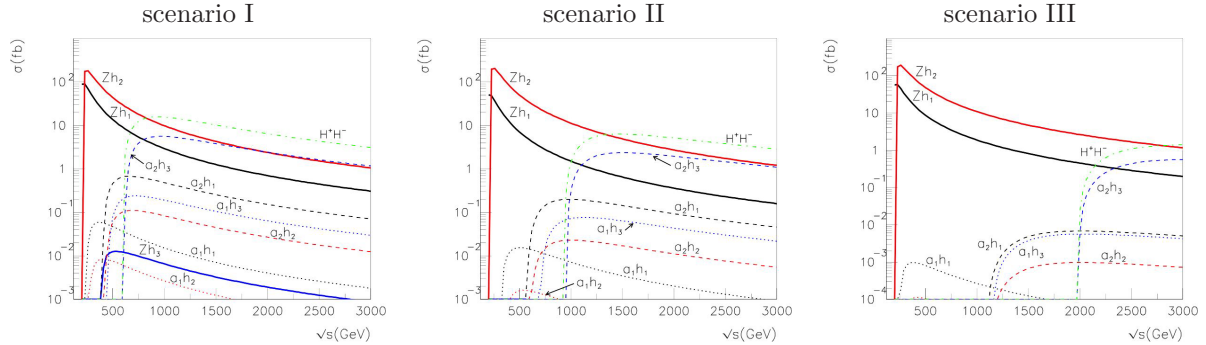


Figure 7: Cross sections for Higgs production at an e^+e^- collider, as functions of the center-of-mass energy \sqrt{s} , for three illustrative mass spectra as tabulated in Table 1. From [15].

Table 1: Higgs masses and LSP mass in GeV for the two scenarios for which we plot e^+e^- cross sections in Fig. 7. Also given are Ωh^2 , the singlino and Higgsino percentages and $R_{gg}^{h_2}(\gamma\gamma)$. Scenarios I) and III) have Ωh^2 in the WMAP window, with I) being typical of the low- $m_{\tilde{\chi}_1^0}$ scenarios and III) being that with smallest m_{h_3} in the large- $m_{\tilde{\chi}_1^0}$ group of points in the WMAP window. Scenario II) is chosen to have m_{a_2} and m_{h_3} intermediate between those for scenario I) and III), a region for which Ωh^2 is substantially below 0.1.

Scenario	m_{h_1}	m_{h_2}	m_{h_3}	m_{a_1}	m_{a_2}	m_{H^\pm}	$m_{\tilde{\chi}_1^0}$	Ωh^2	LSP singlino	LSP Higgsino	$R_{gg}^{h_2}(\gamma\gamma)$
I	99	124	311	140	302	295	76	0.099	18%	75%	1.62
II	97	124	481	217	473	466	92	0.026	20%	74%	1.53
III	99	126	993	147	991	989	115	0.099	75%	25%	1.14

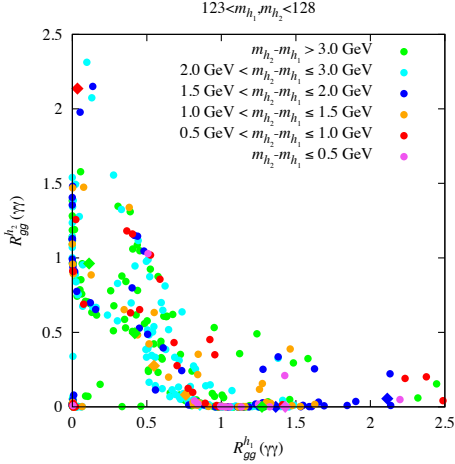


Figure 8: Correlation of $gg \rightarrow (h_1, h_2) \rightarrow \gamma\gamma$ signal strengths when both h_1 and h_2 lie in the 123–128 GeV mass range. Circular points have $\Omega h^2 < 0.094$, while diamond points have $0.094 \leq \Omega h^2 \leq 0.136$. Points are color coded according to $m_{h_2} - m_{h_1}$ as indicated on the figure. From [16].

5 Degenerate case: two Higgses hiding in the 125 GeV signal?

As mentioned, enhanced rates in the $\gamma\gamma$ channel arise in the NMSSM with large λ when the h_1 and h_2 are sufficiently close in mass that one Higgs, h_i , “steals” (through mixing) some of the $b\bar{b}$ width of the other Higgs, h_j . The state with the enhanced $\gamma\gamma$ signal and mass near 125 GeV can be either the h_1 or the h_2 . It is however also possible that h_1 and h_2 both lie in the 123–128 GeV mass window [16]. In this case, a second mechanism for large $\gamma\gamma$ rates emerges — namely both h_1 and h_2 contribute significantly and their summed rate is enhanced even though their individual rates are more or less at, or even somewhat below, the SM level.

Figure 8 shows the correlation of $gg \rightarrow (h_1, h_2) \rightarrow \gamma\gamma$ signal strengths in the semi-constrained NMSSM when both h_1 and h_2 lie in the 123–128 GeV mass range. We see that often one Higgs dominates the signal, but it is also possible that both have $R_{gg}^{h_i}(\gamma\gamma) \gtrsim 0.5$ thus giving a combined signal larger than 1.

To go a step further, we take the net signal in given production and decay channels Y and X to simply be $R_Y^h(X) = R_Y^{h_1}(X) + R_Y^{h_2}(X)$, and we define the resulting “effective” Higgs mass as

$$m_h^Y(X) \equiv \frac{R_Y^{h_1}(X)m_{h_1} + R_Y^{h_2}(X)m_{h_2}}{R_Y^{h_1}(X) + R_Y^{h_2}(X)}. \quad (6)$$

Of course, the extent to which it is appropriate to combine the rates from the h_1 and h_2 depends upon the degree of degeneracy and the experimental resolution. It should be noted that the widths of the h_1 and h_2 are of the same order of magnitude as the width of a 125 GeV SM Higgs boson, *i.e.* they are very much smaller than this resolution.

In Fig. 9, we display in the left-hand plot the strong correlation between $R_{gg}^h(\gamma\gamma)$ and $R_{gg}^h(VV)$, $V = W, Z$. Note that if $R_{gg}^h(\gamma\gamma) \sim 1.5$, as suggested by current experimental results, then in this scenario $R_{gg}^h(VV) \geq 1.2$. In the right-hand plot, we show $R_{gg}^h(\gamma\gamma)$ versus the mass of the lighter pseudoscalar a_1 . It is interesting to note that for the bulk of the points with (quasi-)degenerate $h_{1,2}$ also the other Higgs states tend to be light, with $m_{a_1} \lesssim 300$ GeV and $m_{a_2} \simeq m_{h_3} \simeq m_{H^\pm} \lesssim 500$ GeV.

The scenario again prefers small μ_{eff} of order 100–200 GeV, which is very favorable in point of view of fine tuning, in particular if stops are also light. Indeed a good fraction of our points with degenerate h_1, h_2 and $R(\gamma\gamma) > 1$ features light stops with $m_{\tilde{t}_1} \in [300, 700]$ GeV and $M_{\text{SUSY}} = \sqrt{m_{\tilde{t}_1} m_{\tilde{t}_2}} \lesssim 1$ TeV. Because of the small μ_{eff} , the LSP is dominantly a light higgsino. A relic density of $\Omega h^2 \simeq 0.1$ can be achieved for LSP masses just below 80 GeV, see Fig. 10. The LSP is 70–80% higgsino in this case, with order 20% singlino admixture. The ILC would again be the ideal machine to explore this scenario.

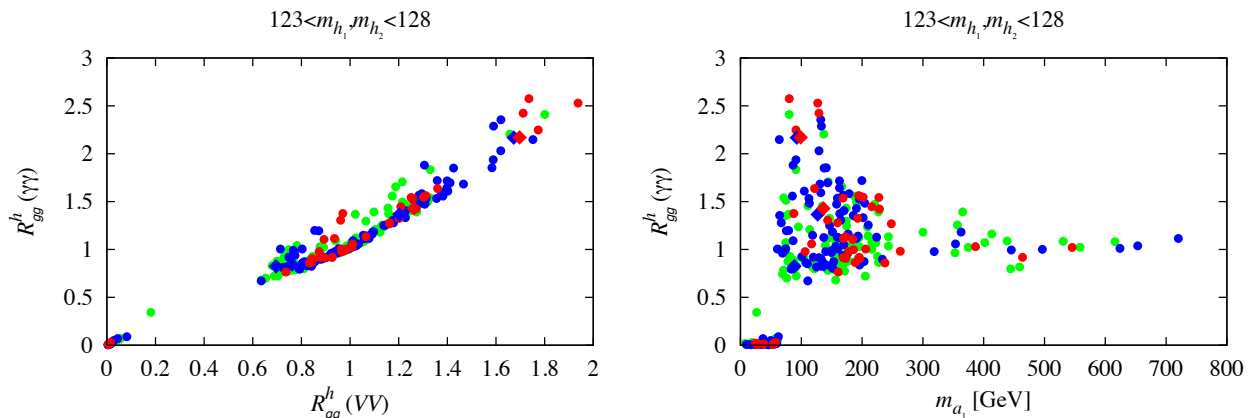


Figure 9: Correlation between the gg induced $\gamma\gamma$ and VV signal strengths (left) and $R_{gg}^h(\gamma\gamma)$ versus the mass of a_1 (right) for NMSSM points with quasi-degenerate h_1 and h_2 in the 123–128 GeV mass window. The green, blue and red points have $\Delta m = m_{h_2} - m_{h_1} = 2\text{--}3$ GeV, $\Delta m = 1\text{--}2$ GeV and $\Delta m \leq 1$ GeV, respectively. From [16].

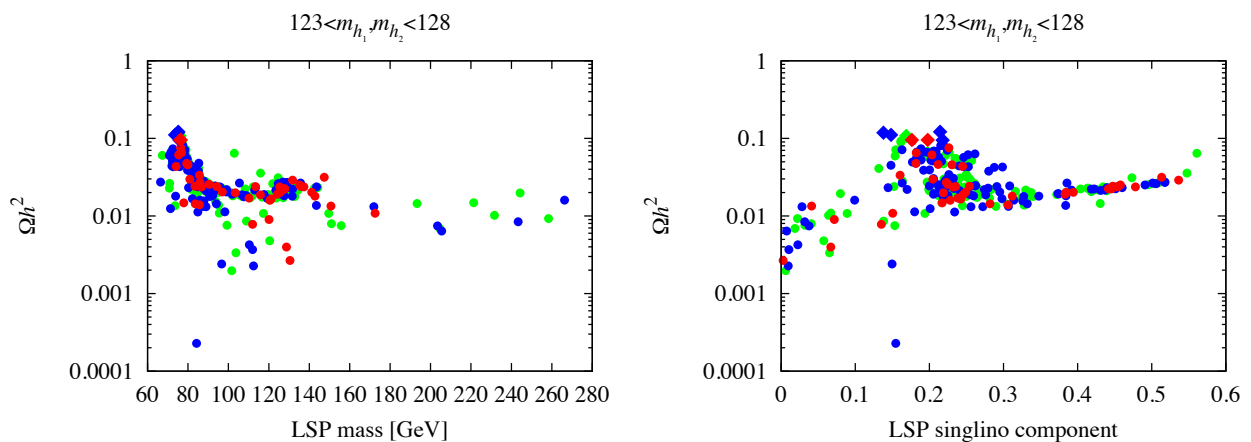


Figure 10: Relic density Ωh^2 versus LSP mass (left) and versus LSP singlino component (right) for NMSSM points with quasi-degenerate h_1 and h_2 in the 123–128 GeV mass window. The green, blue and red points have $\Delta m = m_{h_2} - m_{h_1} = 2\text{--}3$ GeV, $\Delta m = 1\text{--}2$ GeV and $\Delta m \leq 1$ GeV, respectively. From [16].

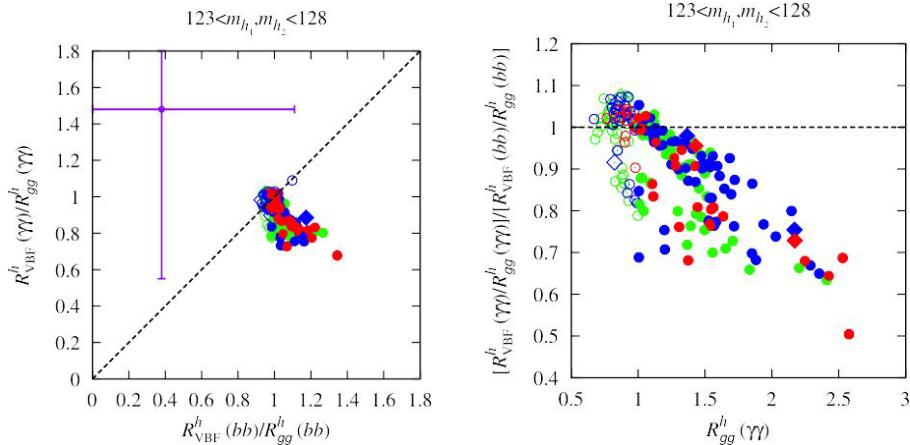


Figure 11: Illustration of the double ratio I) of Eq. (7) for degenerate h_1 and h_2 in the 123–128 GeV mass range in the semi-constrained NMSSM. The green, blue and red points have $\Delta m = m_{h_2} - m_{h_1} = 2\text{--}3$ GeV, $\Delta m = 1\text{--}2$ GeV and $\Delta m \leq 1$ GeV, respectively. From [17].

6 Diagnosing degenerate Higgs bosons

Two or more degenerate Higgs bosons will in general have different relative production rates in the VBF and gg fusion channels for one or more final states. In [17] we thus proposed double ratios of signal strengths as a useful diagnostic tool to reveal the existence of one or more quasi-degenerate (but non-interfering in the small width approximation) Higgs states. For models with Higgs doublets+singlets, the relevant double ratios are:

$$\text{I): } \frac{R_{\text{VBF}}^h(\gamma\gamma)/R_{gg}^h(\gamma\gamma)}{R_{\text{VBF}}^h(b\bar{b})/R_{gg}^h(b\bar{b})}, \quad \text{II): } \frac{R_{\text{VBF}}^h(\gamma\gamma)/R_{gg}^h(\gamma\gamma)}{R_{\text{VBF}}^h(WW)/R_{gg}^h(WW)}, \quad \text{III): } \frac{R_{\text{VBF}}^h(WW)/R_{gg}^h(WW)}{R_{\text{VBF}}^h(b\bar{b})/R_{gg}^h(b\bar{b})}, \quad (7)$$

each of which should be unity if only a single Higgs boson is present but are generally expected to deviate from 1 if two (or more) Higgs bosons are contributing to the net Higgs signals. Values obtained in the semi-constrained NMSSM are shown in Fig. 11.

7 Conclusions

In summary, the observation of the 125 GeV Higgs boson at the LHC has important implications for supersymmetric models. In particular, in the MSSM and NMSSM scenarios discussed here, gluinos and squarks of the first two generations tend to be heavy, in agreement with the non-observation of SUSY signals at the LHC, while stops and EW-inos can be light. Within NMSSM, there exists the intriguing possibility of additional Higgs states in the vicinity of, or degenerate with, the state at 125 GeV. This offers extremely interesting possibilities for precision Higgs physics at the ILC. Neutralinos and charginos are also expected to be light in these scenarios; the lightest states are typically higgsino-like and thus difficult to observe at the LHC. An e^+e^- collider would be the ideal machine to resolve such scenarios.

Acknowledgements

I wish to thank Genevieve Belanger, Felix Brümmer, Beranger Dumont, Ulrich Ellwanger, John F. Gunion, Suchita Kulkarni and Yun Jiang for fruitful and rewarding collaborations, and Gudrid Moortgat-Pick for pushing me to write this contribution. The work presented here was supported in part by IN2P3 under contract PICS FR–USA No. 5872 and by a PEPS-PTI grant “Physique Théorique et ses Interactions”.

References

- [1] G. Aad *et al.* [ATLAS Collaboration], “Observation of a new particle in the search for the Standard Model Higgs boson with the ATLAS detector at the LHC,” *Phys. Lett. B* **716** (2012) 1 [arXiv:1207.7214 [hep-ex]].
- [2] S. Chatrchyan *et al.* [CMS Collaboration], “Observation of a new boson at a mass of 125 GeV with the CMS experiment at the LHC,” *Phys. Lett. B* **716** (2012) 30 [arXiv:1207.7235 [hep-ex]].
- [3] G. Cacciapaglia, A. Deandrea, G. D. La Rochelle and J. -B. Flament, “Higgs couplings beyond the Standard Model,” *JHEP* **1303** (2013) 029 [arXiv:1210.8120 [hep-ph]].
- [4] G. Belanger, B. Dumont, U. Ellwanger, J. F. Gunion and S. Kraml, “Higgs Couplings at the End of 2012,” *JHEP* **1302** (2013) 053 [arXiv:1212.5244 [hep-ph]].
- [5] A. Djouadi, “The Anatomy of electro-weak symmetry breaking. II. The Higgs bosons in the minimal supersymmetric model,” *Phys. Rept.* **459** (2008) 1 [hep-ph/0503173].
- [6] F. Brummer, S. Kraml and S. Kulkarni, “Anatomy of maximal stop mixing in the MSSM,” *JHEP* **1208** (2012) 089 [arXiv:1204.5977 [hep-ph]].
- [7] <https://twiki.cern.ch/twiki/bin/view/AtlasPublic/SupersymmetryPublicResults>.
- [8] <https://twiki.cern.ch/twiki/bin/view/CMSPublic/PhysicsResultsSUS>.
- [9] For a review, see *e.g.* U. Ellwanger, C. Hugonie and A. M. Teixeira, “The Next-to-Minimal Supersymmetric Standard Model,” *Phys. Rept.* **496** (2010) 1 [arXiv:0910.1785 [hep-ph]].
- [10] J. F. Gunion, Y. Jiang and S. Kraml, “The Constrained NMSSM and Higgs near 125 GeV,” *Phys. Lett. B* **710** (2012) 454 [arXiv:1201.0982 [hep-ph]].
- [11] U. Ellwanger, “Enhanced di-photon Higgs signal in the Next-to-Minimal Supersymmetric Standard Model,” *Phys. Lett. B* **698** (2011) 293 [arXiv:1012.1201 [hep-ph]].
- [12] U. Ellwanger, “A Higgs boson near 125 GeV with enhanced di-photon signal in the NMSSM,” *JHEP* **1203** (2012) 044 [arXiv:1112.3548 [hep-ph]].
- [13] U. Ellwanger and C. Hugonie, “Higgs bosons near 125 GeV in the NMSSM with constraints at the GUT scale,” *Adv. High Energy Phys.* **2012** (2012) 625389 [arXiv:1203.5048 [hep-ph]].
- [14] <http://www.th.u-psud.fr/NMHDECAY/nmssmtools.html>.
- [15] G. Belanger, U. Ellwanger, J. F. Gunion, Y. Jiang, S. Kraml and J. H. Schwarz, “Higgs Bosons at 98 and 125 GeV at LEP and the LHC,” *JHEP* **1301** (2013) 069 [arXiv:1210.1976 [hep-ph]].
- [16] J. F. Gunion, Y. Jiang and S. Kraml, “Could two NMSSM Higgs bosons be present near 125 GeV?,” *Phys. Rev. D* **86** (2012) 071702 [arXiv:1207.1545 [hep-ph]].
- [17] J. F. Gunion, Y. Jiang and S. Kraml, “Diagnosing Degenerate Higgs Bosons at 125 GeV,” *Phys. Rev. Lett.* **110** (2013) 051801 [arXiv:1208.1817 [hep-ph]].